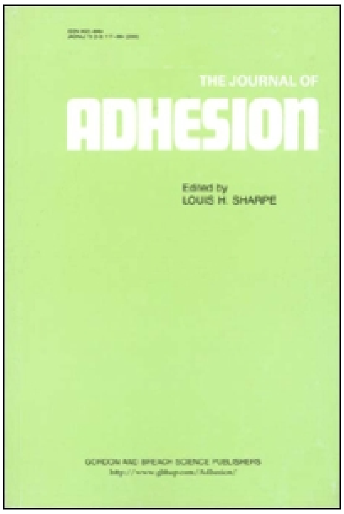

The Journal of Adhesion
Publication details, including instructions for authors and subscription information:
http://www.informaworld.com/smpp/title~content=t713453635

Stress Corrosion Cracking of Adhesive Joints

E. J. Ripling[a]; S. Mostovoy[a]; C. Bersch[b]
[a] Materials Research Laboratory, Inc., Glenwood, Illinois, U.S.A. [b] Naval Air Systems Command, Washington, D.C., U.S.A.

To cite this Article Ripling, E. J. , Mostovoy, S. and Bersch, C.(1971) 'Stress Corrosion Cracking of Adhesive Joints', The Journal of Adhesion, 3: 2, 145 — 163
To link to this Article: DOI: 10.1080/00218467108081160
URL: http://dx.doi.org/10.1080/00218467108081160

J. Adhesion, 1971, Vol. 3, pp. 145–163

Printed in Northern Ireland

Stress Corrosion Cracking of Adhesive Joints[†]

E. J. RIPLING, S. MOSTOVOY

Materials Research Laboratory, Inc., Glenwood, Illinois, U.S.A.

C. BERSCH

Naval Air Systems Command, Washington, D.C., U.S.A.

(*Received November* 24, 1970)

The limiting long time static load carrying capability of an epoxy joint was found to depend on its ability to resist crack extension in the presence of water. This resistance to crack extension in an aggressive environment can be quantitatively described as the threshold of crack-extension-force below which stress corrosion cracking cannot occur, i.e. $\mathscr{G}_{ISCC}$. It was found for DER 332 hardened with TEPA that $\mathscr{G}_{ISCC}$ was approximately $\frac{1}{3}$ to $\frac{1}{2}$ $\mathscr{G}_{IC}$, the crack-extension-force in short times in the absence of water. The same resin hardened with HHPA had a value of $\mathscr{G}_{ISCC}$ that could be as low as 1/10 $\mathscr{G}_{IC}$ for the same system.

For a particular resin system, $\mathscr{G}_{ISCC}$ was also found to be a function of relative humidity

INTRODUCTION

Recurring honeycomb failures on many types of aircraft underscore the need for a way to predict the performance of adhesive bonds when they are exposed to long term loading, both static and dynamic, in aggressive environments such as heat and water vapor. The concepts of fracture mechanics and the experimental versatility of the tapered double cantilever beam (TDCB) may satisfy that need.

Service fractures of structural adhesive bonds generally occur in two steps; a pre-existing, crack-like flaw that is introduced accidentally in manufacturing or service first grows slowly to its critical size, after which complete

---

[†] First presented at the 2nd National SAMPE Technical Conference; Dallas, Texas, October 6–8, 1970. Copies of the preprint book may be purchased for $30 from SAMPE National Business Office, Azusa, California 91702.

separation occurs abruptly. Slow, sub-critical crack growth is associated with either fatigue, stress-corrosion-cracking, or a combination of both. Rapid cracking, of course, is associated with the instantaneous attainment of a critical load.

The previous paper has described how one associates the critical load and flaw size at which fast fracture will occur[5]. It is described by $\mathscr{G}_{IC}$, the critical crack extension force or fracture toughness. This paper concentrates on slow crack growth, resulting from the combination of long term static loading and the aggressive action of water in liquid or vapor form. The important value of crack extension force in this case is $\mathscr{G}_{ISCC}$, the threshold value of $\mathscr{G}_i$ below which stress corrosion crack extension will not occur. No results are presented for the influence of dynamic loading or heat, since available resources have been focussed on the static load-water combination. Preliminary studies suggest that the effects of dynamic loading are similar to, but more severe than those for static loading.

MATERIALS AND TEST PROCEDURE

The stress corrosion cracking (SCC) characteristics of two epoxy adhesive systems were studied in the presence of water, in both liquid and vapor form, while under both short time, and long time, static loading. The adhesive systems both used the same resin. DER 332, with two different types of hardener: TEPA a room temperature curing amine, and the other, HHPA, a high temperature curing anhydride. Hardener content and post-cure temperature were varied as described below. Post-curing was done for five hours in all cases and bond thickness was 5 mils unless otherwise noted.

The adherends were half-inch thick plates of the aluminum alloy, 2024-T361, cut to form tapered cantilever beams. The methods for preparing specimens and for conducting tests, to evaluate both toughness and stress corrosion cracking, have been described in detail previously[1-5].

TOUGHNESS OF ADHESIVES IN THE PRESENCE OF WATER

To separate the influence of the variables, water and time under load, on the long term load carrying capacity of adhesive joints requires first a description of the influence of water on short time loading. Changes in fracturing behavior in short times, i.e., under conditions of rapid crack extension, are evaluated by changes in toughness where toughness is defined as the critical value of crack-extension-force $\mathscr{G}_{IC}$. For the TDCB specimen, $\mathscr{G}_{IC}$ is proportional to the square of the critical load, P_c, at which rapid crack extension is initiated[1]. Hence, the influence of water on rapid fracturing is apparent from the shape of the load, P, vs. displacement, Δ, curve. The effect of water was studied by loading a specimen to its critical value in one environment to evaluate $\mathscr{G}_{IC}$, unloading it, changing the environment, reloading it to obtain another value of $\mathscr{G}_{IC}$ in the new environment, etc.

TEPA Hardened System

The studies on toughness of TEPA hardened epoxy joints showed that two types of P-Δ curves could be obtained, depending on the combination of post-cure temperature and hardener-to-resin content[2,5]. With high-cure temperatures and high hardener contents, the P-Δ curve showed two distinct instability points, Figure 1-a. The upper critical load, P_c, is associated with the toughness required to cause a stationery or slow extending crack to abruptly jump ahead, while the lower one, P_a, is associated with the crack arrest toughness, $\mathscr{G}_{IA}$, the value of crack-extension force at which a running crack is stopped.

At low post-cure temperatures, and low hardener contents, the initiation and arrest toughness are identical, Figure 1-b. For these materials cracking is stable, and the cracking rate is proportional to the velocity of the test machine cross-head.

Adhesives hardened with TEPA were selected to represent both stable and unstable cracking under increasing loads. The adhesive used for the former was 10T/180† and for the latter, 12.5T/270. The effect of water on the stable cracking adhesive, 10T/180, is shown by the series of P-Δ diagrams in Figure 2. Since, for the specimen used, crack length a was proportional to Δ at constant P, the $\mathscr{G}$ was proportional to P^2, a and $\mathscr{G}$ are also indicated in the abscissa and ordinate of this chart. The specimen was first pre-cracked to slightly more than two inches, after which it was tested to obtain a value of $\mathscr{G}_{IC}$ in the absence of water (curve 1). The crack was extended as additional inch in the course of this test, and a value of $\mathscr{G}_{IC}$ of approximately 0.30 lbs/in. was obtained. The specimen was then unloaded, stored three days in 50 percent relative humidity (R.H.) after which it was retested (curve 2). Storage increased the initiation toughness to a value of about 0.34 lbs/in., but the improved toughness was localized to the vicinity of the crack tip. After the crack had advanced some short distance, $\mathscr{G}_{IC}$ reverted

---

† Adhesives are identified as follows:
First number = PHR of hardener
Letter = hardener, T = TEPA and H = HHPA
Second number = post-cure temperature in °F for five hours

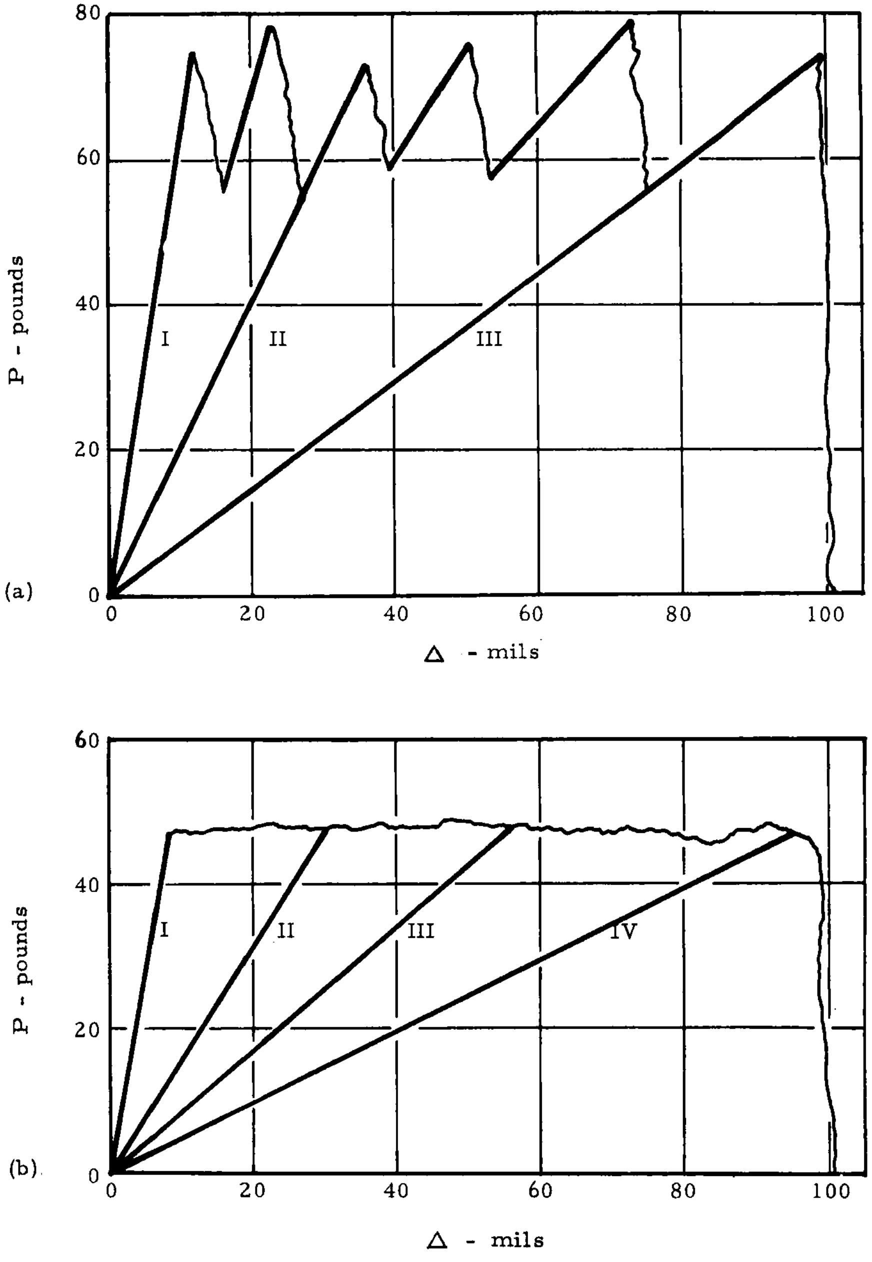

FIGURE 1 Schematic P-Δ curves. (a) Unstable cracking, (b) Stable cracking.

to its original value ($\approx$ 0.30 lbs/in.). The specimen whose crack length was now approximately four inches was again unloaded, stored 17 hours in 100 percent R.H. and retested (curve 3). The more humid storage further increased $\mathcal{G}_{\mathrm{IC}}$ to about 0.39 lbs/in. and in this case the improved toughness persisted so that a second "pop" was experienced in crack extension. Some increased toughness even persisted during the stable cracking that followed the "pops". The specimen was again unloaded, and water was introduced to the crack tip for a five minute storage.

On reloading (curve 4) some model toughening again occurred. Finally,

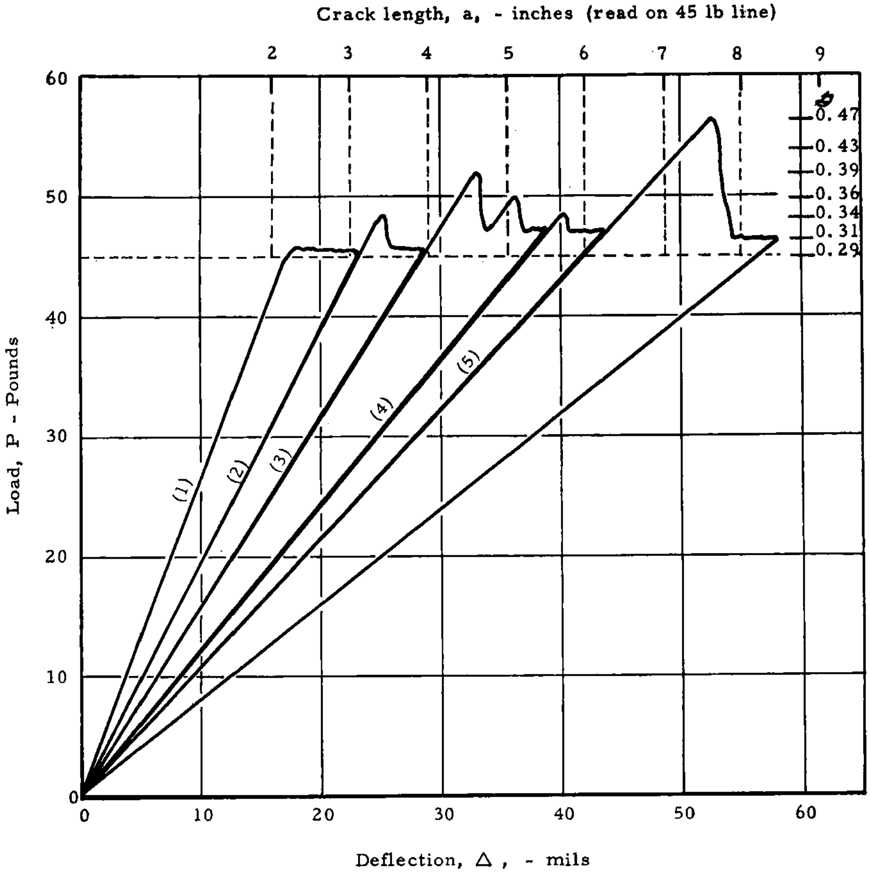

FIGURE 2 P-Δ records for 10T/180 adhesive specimen tested: (1) Immediately after precracking, (2) After three day storage in 50% R.H., (3) After 17 hour storage in 100% R.H., (4) After introducing water into the crack and storing five minutes, (5) Same as 4 with wetting agent (0.05 w/o Kodak photoflo) added to water. (Cross-head rate 1.0 in./min.). Ref. 3.

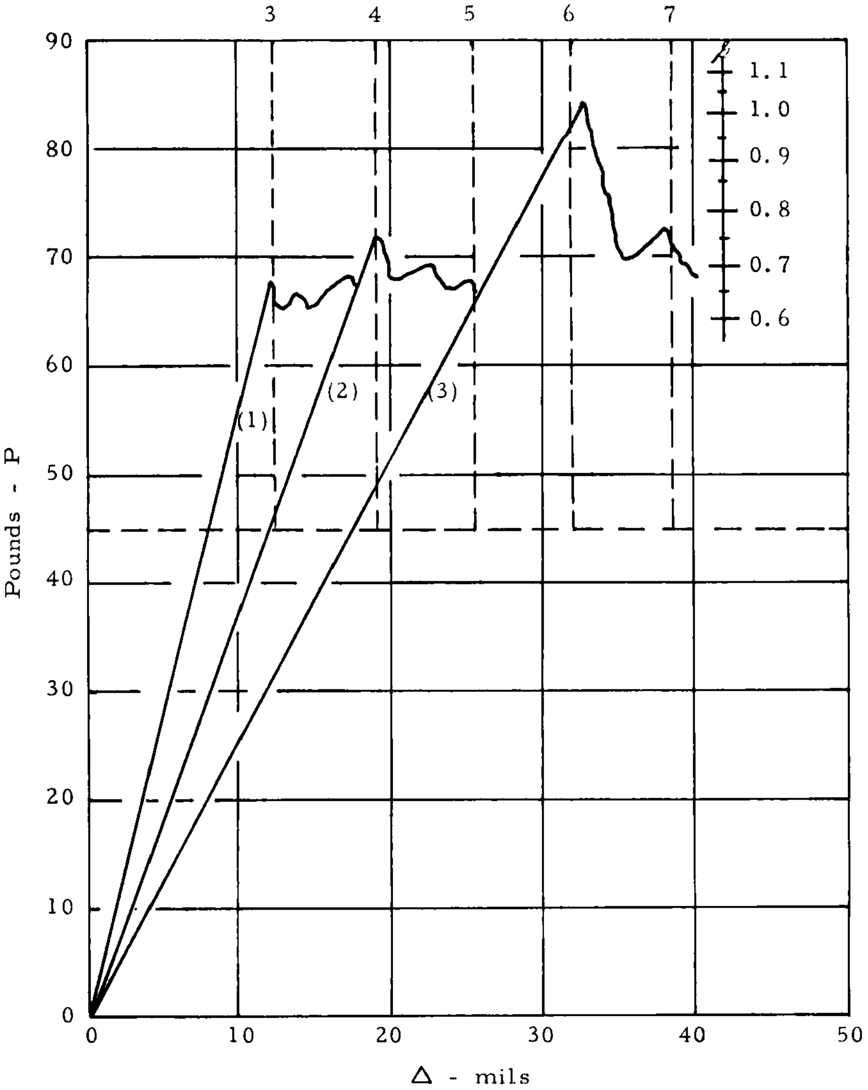

FIGURE 3 P-Δ records for 70H/311 adhesive specimen tested: (1) Dry—immediately after precracking, (2) after 10 minutes in water with wetting agent, (3) After 2 hours in water with wetting agent. Ref. 7.

the specimen was again unloaded, water again introduced into the crack tip for five minutes, but in this case a wetting agent was added to the water, (0.05 w/o Kodak Photo-Flo). On subsequent reloading (curve 5), the toughness was markedly improved to a $\mathscr{G}_{IC} = 0.47$ lbs/in. Again, the large improvement was restricted to the first "pop". It is seen that water toughens the crack tip over such a small distance that the initiation toughness is increased but $\mathscr{G}_{IA}$ is essentially unaffected.

The same sort of tests were conducted with the 12.5T/270 adhesive specimens. These showed a great deal more scatter in initiation toughness than the 10T/180 specimens in the absence of water, and the influence of water on $\mathscr{G}_{IC}$, if any, was masked within the scatter band. In any event, the 12.5T/270 was far less influenced by water than was the 10T/180.

HHPA Hardened System

Unlike the TEPA hardened adhesives, the HHPA systems produced unstable *P*-Δ curves for all combinations of hardener-to-resin content and post-cure temperature[5]. Consequently, the influence of water on short time loading was examined for only a single adhesive. 70H/311. Because water plus a wetting agent had the largest influence on $\mathscr{G}_{IC}$, for the TEPA system, only this single environment was used for the HHPA system. The *P*-Δ curves for this adhesive are shown in Figure 3. The specimen was again first fractured dry to establish $\mathscr{G}_{IC}$ in the absence of water. The dry toughness as shown by curve 1 was $\mathscr{G}_{IC} = 0.63$ to 0.68 lbs/in. Unloading the specimen, storing it ten minutes in water with the wetting agent, and retesting resulted in a value of $\mathscr{G}_{IC}$ slightly above 0.70 lbs/in. (curve 2). Repeating the unloading and reloading after two hours storage in water with wetting agent (curve 3) increased $\mathscr{G}_{IC}$ to approximately 1.0 lbs/In. The increased toughness persisted for one to 1½ inches and then reverted back to its value of 0.63 to 0.68 lbs/in. Still longer exposure (10 hours) to water prior to testing decreased the toughness due to a change in fracture morphology as discussed below.

STRESS CORROSION CRACKING

Crack Morphology

When pre-cracked specimens were subjected to sustained loading in the presence of either humid air or liquid water, both their load carrying capacity was reduced and their fracture morpthology was changed. For specimens loaded so that they failed in one to two minutes or less, cracking of thin adhesive bonds always occurred cohesively near the center-of-the-bond (CoB) so long as the bond was properly made and the amount of hardener was not excessive. For pre-cracked specimens exposed to loads less than the critical load to cause rapid cracking, i.e., $\mathscr{G}_i < \mathscr{G}_{IC}$, in either liquid water or humidities above a few percent, the crack extended at or near one or both interfaces (IF). Hence, if a specimen were subjected to the following stress history: fast fracture by a continuously increasing load, then exposure to humidity at $\mathscr{G}_i < \mathscr{G}_{IC}$ where slow cracking occurred, and finally fast fracture again, the crack morphology would be CoB, IF and again CoB as shown in Figure 4. Further, the IF fracture is not continuous with the CoB crack.

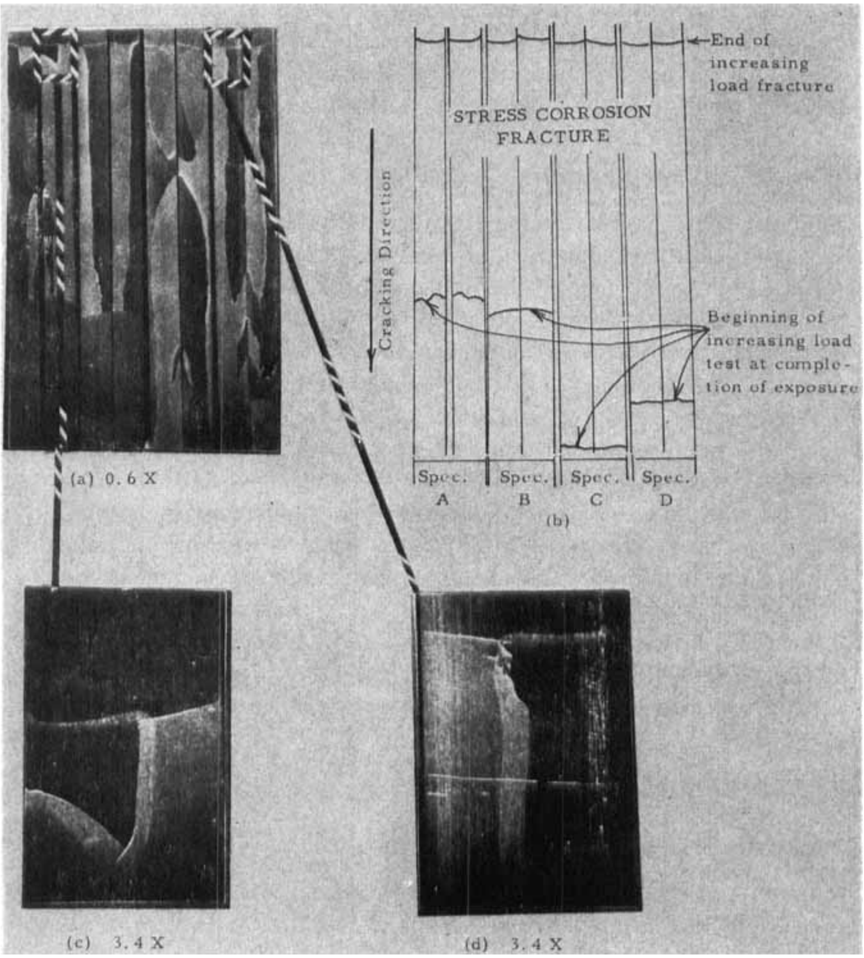

FIGURE 4 Fracture surface of 10T/180 adhesive after 100 hour exposure at 96% R.H. (a) Four specimens showing various crack extension lengths during test (low magnification); (b) Schematic drawing of (a); (c) and (d) Increased magnification showing double debonding Ref. 3.

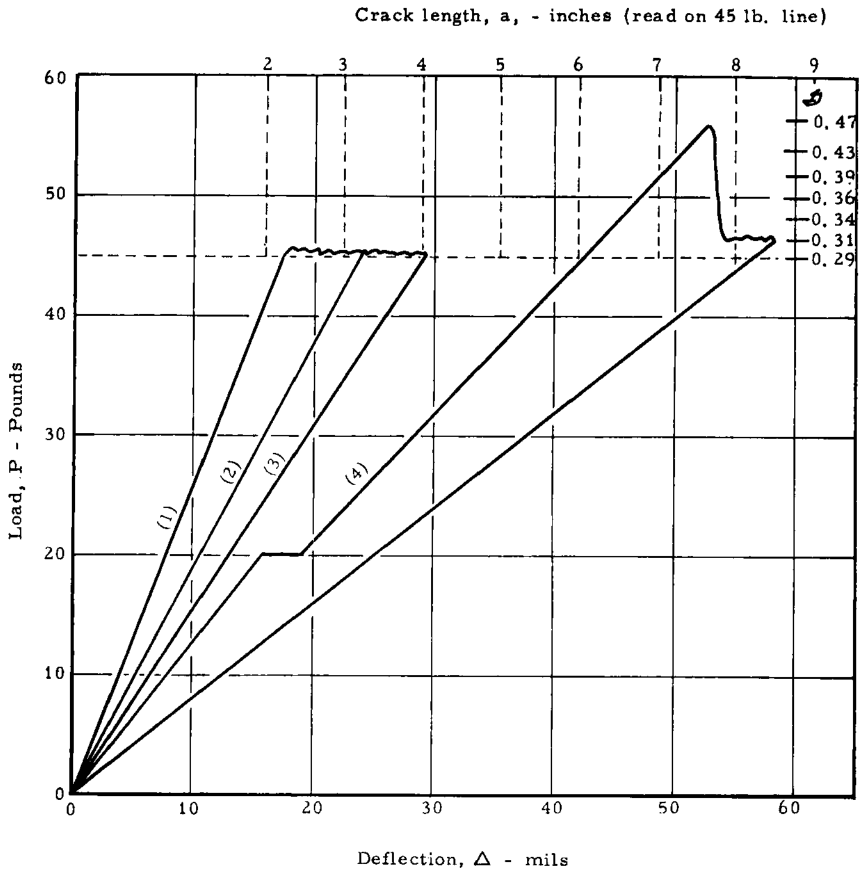

FIGURE 5 Increasing load P-Δ records for 10T/180 adhesive specimen tested before and after 100 hour exposure to a high $\mathscr{G}$. (a) Tested immediately after precracking, (2) Retested, (3) Unloaded for exposure, (4) Retested after exposure. Ref. 3.

Instead, the IF crack starts at the air-adhesive-adherend interface immediately above or below the CoB crack tip (see Figure 6). The crack extends from the edges until it is across the full thickness of the specimen. If the cracks growing from the two edges do not lie in the same plane, i.e., one is on the "top" of the adhesive layer, and the other is on the "bottom", double debonding will occur. The white layers in the photograph of Figure 4-a are such double debonded areas, and these are more clearly seen in Figures 4-c and d. The crack, in growing in from the edges also caused debonding for some small distance under the CoB pre-crack. This is also apparent in Figures 4-c and d. Because the CoB and IF cracks are not continuous, there is an unbroken connecting ligament between the CoB and IF fracture surfaces even after the IF crack has grown some considerable distance. Evidence of the existence of this unbroken ligament is sometimes found in specimens that are tested rapidly after having first been CoB and IF cracked. The specimen in Figure 5 was tested twice in the dry condition to obtain curves 1 and 2. After unloading (curve 3), it was exposed for 100 hours in 96 percent R.H. at a value of $\mathscr{G}_{\mathrm{i}}$ just less than $\mathscr{G}_{\mathrm{IC}}$. During exposure the crack extended IF, and on subsequent testing, the elastic P-Δ curve showed a step. The slope of the curve before and after the step is quite different. Prior to the step, the unbroken ligament between the CoB and IF crack is carrying most of the load so that the specimen compliance indicates a short crack. After the ligament breaks, the compliance abruptly increases because the crack length is now given by the end of the IF region.

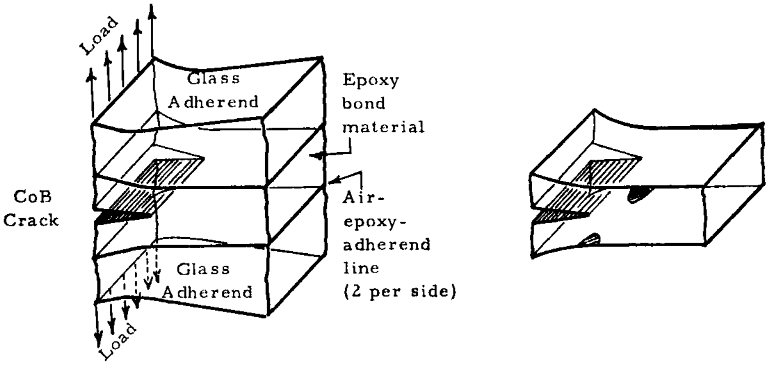

(a) Section of tapered glass adherends adhesive specimen with increasing load CoB fracture prior to stress corrosion exposure.

(b) Bond section only showing two static fatigue cracks both formed at lower interface-air boundary and propagating toward one another. (These cracks may be formed on opposite interfaces on occasion.)

(c) Successive stages of crack extension before link up.

(d) Link up of interface crack and successive propagation. Note that end of CoB crack does not link up with interface crack. (Start of interface crack may occur slightly behind CoB crack.)

FIGURE 6 Schematic drawing of stress corrosion crack extension. Ref. 3.

Some tests were also made using glass adherends so that the crack tip could be observed directly. Lapsed time movies were made of the crack extending by stress corrosion, and a schematic drawing of the chronology of cracking is given in Figure 6. This drawing essentially summarizes the crack morphology associated with cracking of all the adhesives tested: CoB cracking with fast cracking and IF with SCC.

$\mathcal{G}_{\mathrm{ISCC}}$ of TEPA Hardened System

To evaluate $\mathcal{G}_{\mathrm{ISCC}}$, the threshold of $\mathcal{G}_{\mathrm{i}}$ below which SCC will not occur in a reasonable time, specimens were exposed to a variety of relative humidities and to liquid water (plus wetting agent) at values of $\mathcal{G}_{\mathrm{i}} < \mathcal{G}_{\mathrm{IC}}$. The crack length, a, was monitored for each humidity and load, as a function of exposure time. Since, for the TDCB specimen, a is proportional to the displacement at the loading holes, Δ, collecting data of this type is straightforward. A typical record of a vs. time is shown in Figure 7. In all cases the

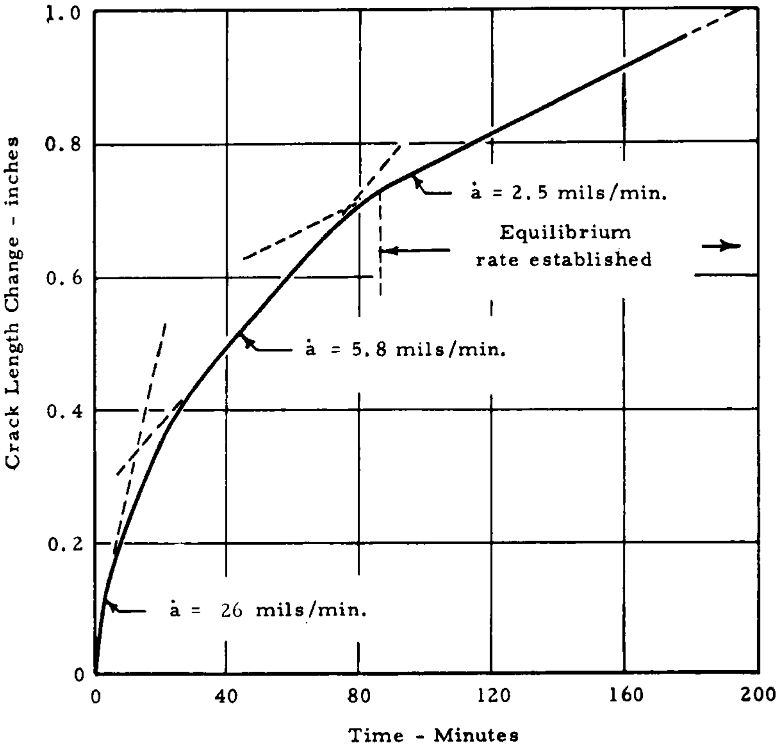

FIGURE 7 Typical crack extension record obtained on 12.5T/270 adhesive specimen exposed to liquid water. Ref. 3.

test at each value of $\mathcal{G}_i$ was continued until an equilibrium cracking rate was obtained. If no crack extension could be detected in three to four hours, the crack growth rate, $\dot{a}$, was assumed less than 0.01 mils/min. The values of $\dot{a}$ obtained from curves of the type shown in Figure 7 were plotted as a function of applied crack-extension-force $\mathcal{G}_i$, for each environment, as shown in Figure 8. The curve of $\dot{a}$ vs. $\mathcal{G}_i$ was then plotted as the upper bound

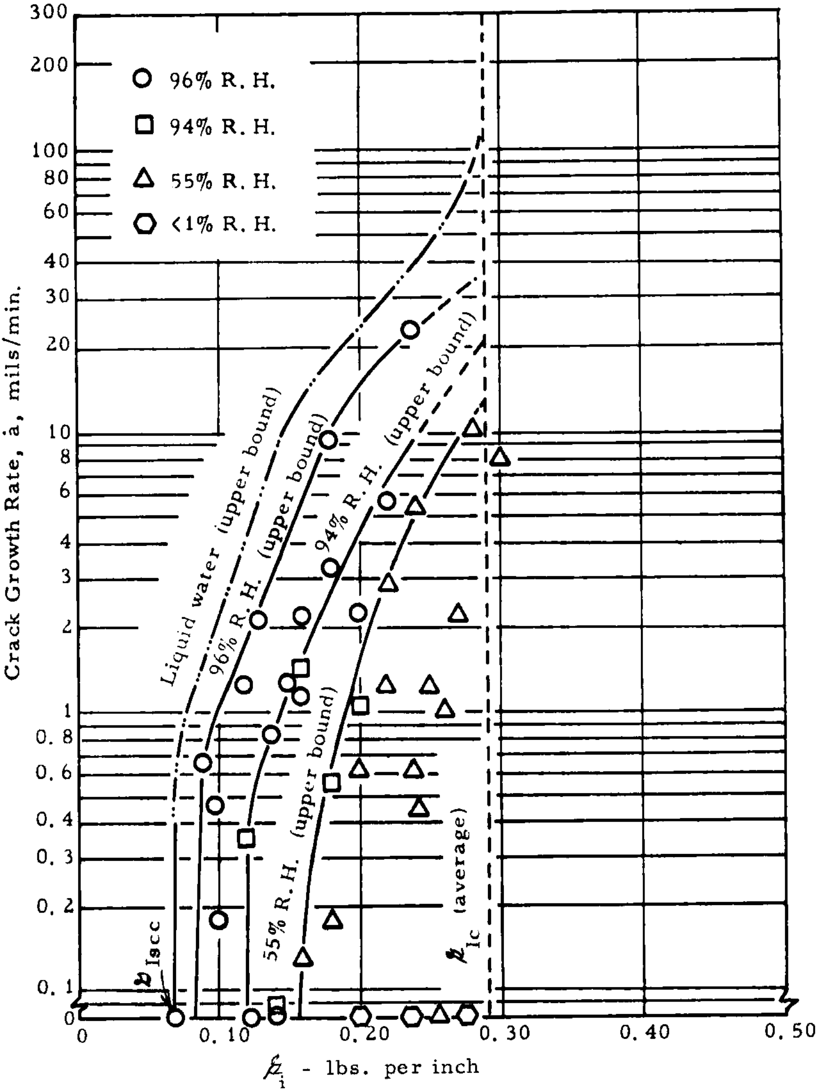

FIGURE 8 Stress Corrosion cracking of 10T/180 adhesive as a function of relative humidity. Ref. 3.

for each exposure condition. The intersection of these curves with the abscissa gave the values of $\mathscr{G}_{ISCC}$.

For 10T/180, $\mathscr{G}_{ISCC}$ is seen to be a function of relative humidity, approaching as its limit the value of $\mathscr{G}_{ISCC}$ for liquid water. For the highest humidity (96 percent R.H.), or liquid water $\mathscr{G}_{ISCC}$ is approximately 0.08 lbs/in., while the average value of $\mathscr{G}_{IC}$ was 0.29 lbs/In. The presence of water reduced the useable toughness of the joint by about 70 percent. At ambient humidity

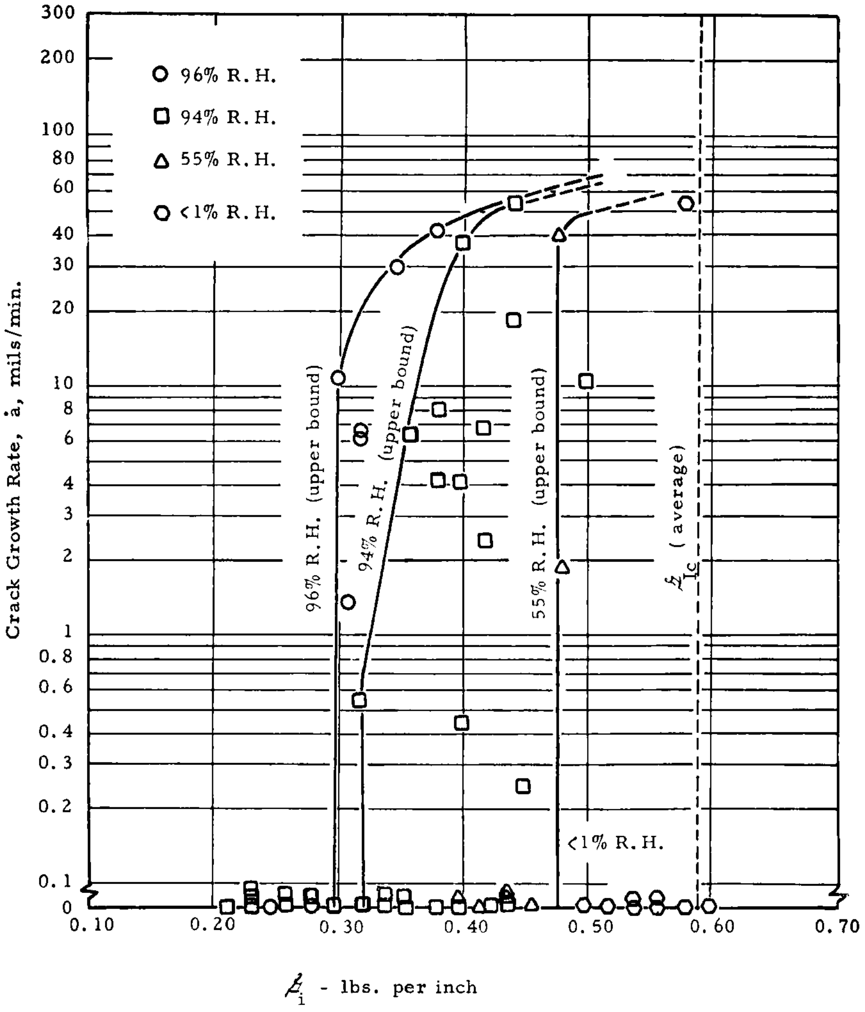

FIGURE 9 Stress corrosion cracking of 12.5T/270 adhesive as a function of relative humidity. Ref. 3.

(55 percent R.H.) $\mathscr{G}_{ISCC}$ is increased to about $\mathscr{G}_{IC}/2$; and if the joint were kept dry (i.e., 0.1 percent R.H.), its long time load carrying capacity could approach the short time value, $\mathscr{G}_{IC}$. Obviously, the reduction in long time load carrying capacity of adhesive joints must be attributed to the influence of water.

Similar tests were conducted on the 12.5T/270 adhesive, Figure 9. The behavior for this adhesive was similar to that of the 10T/180. The value of $\mathscr{G}_{ISCC}$ was again a function of R.H., and again liquid water appeared to be the upper bound for cracking rate and lower bound for $\mathscr{G}_{ISCC}$ as the humidity was increased. Even in the presence of 96 percent R.H. or liquid water, however, $\mathscr{G}_{ISCC}$ for this adhesive was reduced only to $\mathscr{G}_{IC}/2$. Hence, 12.5T/270 was not only less affected by water in a fast test, but its sensitivity to water, under sustained loading was also less than that of 10T/180.

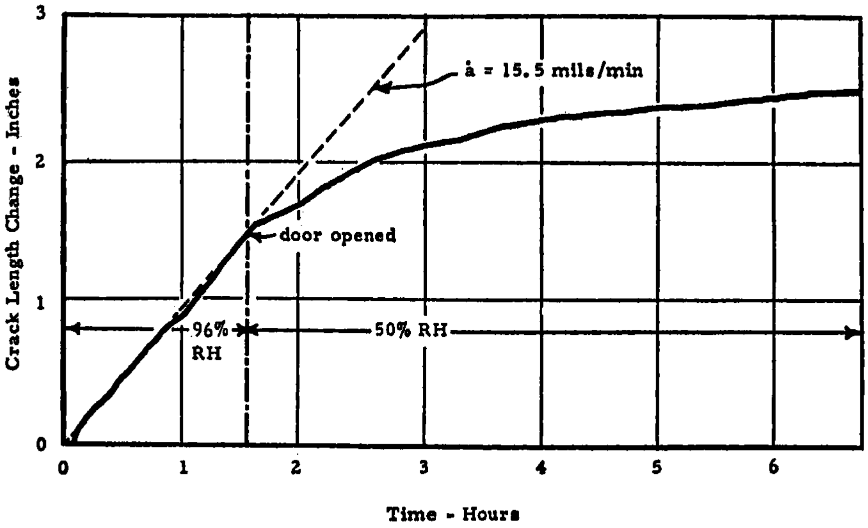

FIGURE 10 Stress corrosion cracking of a 12.5T/270 adhesive specimen exposed first to 96% R.H. and then 50% R.H. at $\mathscr{G}$ = 0.32 lbs/in. Ref. 3.

To demonstrate the effectiveness of humidity on $\dot{a}$ and $\mathscr{G}_{ISCC}$, a specimen of 12.5T/270 was loaded to a $\mathscr{G}_i$ value between $\mathscr{G}_{ISCC}$ for 50 and 96% R.H. (i.e., $\mathscr{G}_i$ = 0.32 lbs/in.). The specimen was then exposed to 96 percent R.H. and the crack length monitored, Figure 10. After the crack grew about $1\frac{1}{2}$ inches in the high humidity, the door of the humidity cabinet was opened so that the humidity dropped to ambient (50 percent R.H.). As the humidity decreased, $\dot{a}$ decreased, and eventually stopped.

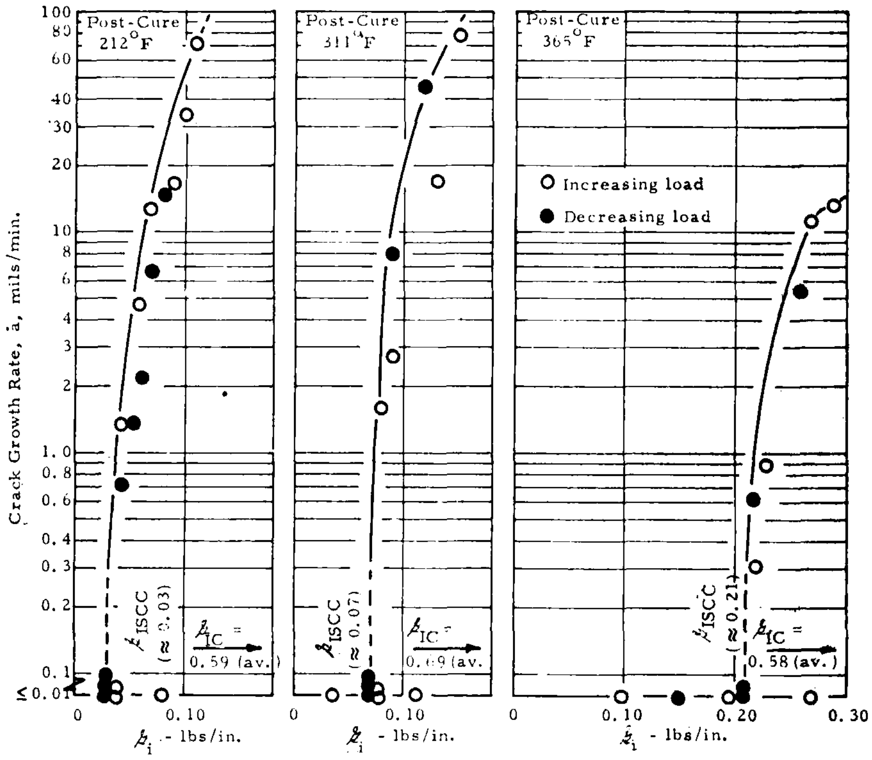

FIGURE 11 Stress corrosion cracking of 5 mil. 20 PHR HHPA adhesive bond in liquid water with wetting agent. Ref. 7.

$\mathcal{G}_{ISCC}$ of HHPA Hardened System

The SCC characteristics of HHPA hardened adhesive were also investigated. Three ratios of hardener-to-resin content were selected; two having less hardener than stoichiometric (84 PHR), i.e., 50 and 70 PHR, and one above stoichiometric (120 PHR). For each composition, three post-cure temperatures were also used; two in the normally used range, i.e., 212 and 311 °F, and one above this range, i.e., 365°F. Two compositions below stoichiometric and the higher post-cure temperature were chosen because, based on TEPA data, these specimens were expected to give higher values of $\mathcal{G}_{ISCC}$ than those post-cured in the normal range having compositions of stoichiometric or above. Because liquid water with a wetting agent appeared to represent the upper limit of cracking rates with increased humidity for the TEPA hardened system, only this environment was used with the HHPA hardened system. The shape of the $\dot{a}$ vs. $\mathcal{G}_i$ curves for this system, as shown by the typical data in Figure 11, was similar to that of the TEPA system. The anhydride hardened epoxy was more damaged by water than the amine hardened one, however.

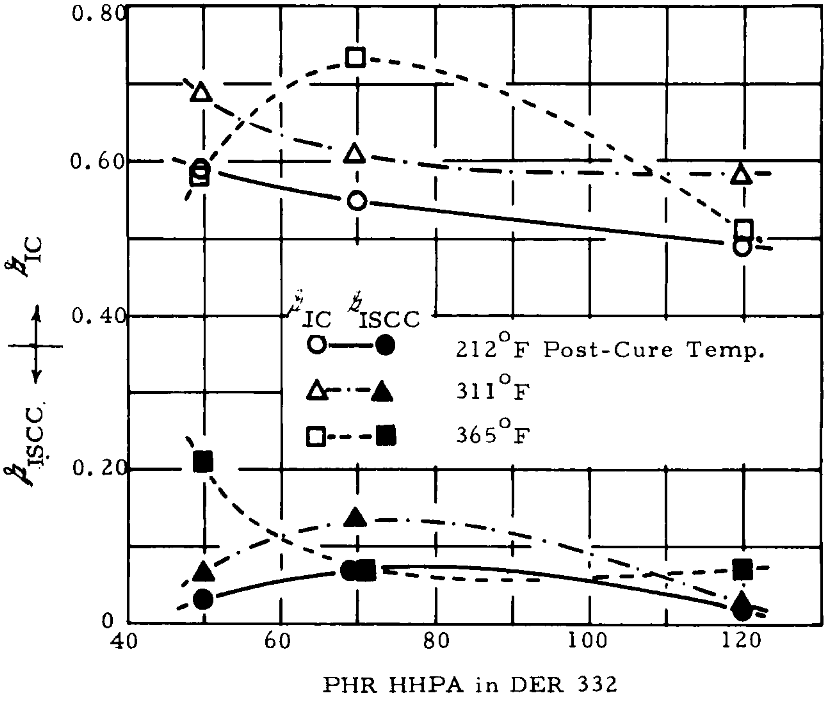

FIGURE 12 Comparison of $\mathcal{G}_{IC}$ and $\mathcal{G}_{ISCC}$ of HHPA hardened epoxy joints.

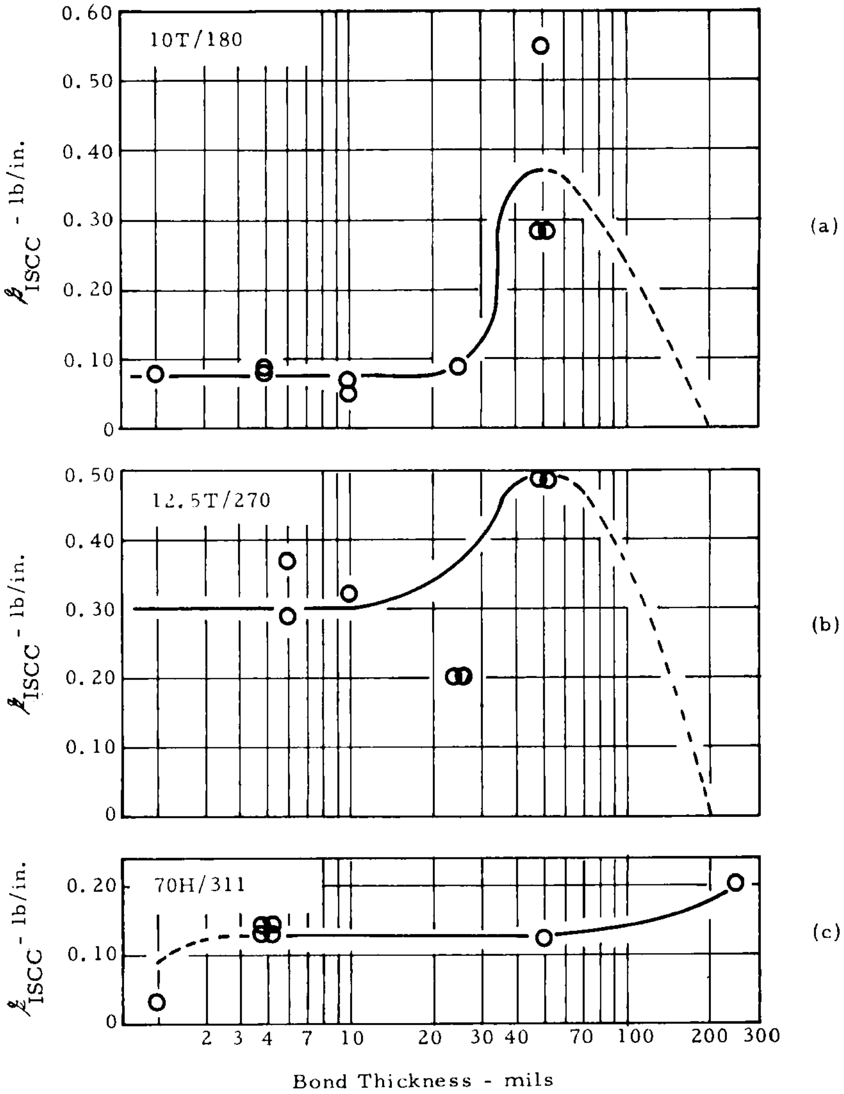

FIGURE 13 Effect of bond thickness on $\mathscr{G}_{ISCC}$ for the three adhesives (a) 10T/180, (b) 12.5T/270, and (c) 70H/311. Ref. 6.

Whereas for the amine system the ratio of $\mathscr{G}_{ISCC}$ to $\mathscr{G}_{IC}$ was of the order of 1/4 to 1/2, for the anhydride system it might be less than 1/10. This severe sensitivity to water on long time loading is shown by the summary curves in Figure 12. The least sensitive material to SCC, 50H/365, had a ratio of

$\mathcal{G}_{ISCC}$ to $\mathcal{G}_{IC}$ of about 1/3 while the most sensitive, 50H/212 or 120H/212, had ratios of less than 1/10.

EFFECT OF JOINT THICKNESS ON SCC

The toughness of joints hardened with either TEPA or HHPA was found to increase with joint thickness so long as the joint continued to fracture CoB[6]. For the TEPA hardened system, fracturing switched from CoB to IF for thicknesses greater than 45 to 60 mils, and joints greater than 100 mils could not be prepared because they separated on cooling from the post-cure temperature. For HHPA, IF fracturing did not occur until the joint thickness was greater than 200 mils and even then, IF fractures were rare. So long as CoB fracturing occurred, $\mathcal{G}_{IC}$ continued to increase for anhydride hardened joints even as thick as 250 mils. The increased toughness for all of these thick joints was associated with an increasing level of macro-roughening of the fracture surface that began to occur at about 25 mils.

Since SCC always occurred IF, there was no opportunity for the crack morphology to change with joint thickness. Hence SCC as a function of joint thickness for 10T/180, 12.5T/270 and 70H/311 was evaluated. The values of $\mathcal{G}_{ISCC}$ are summarized in Figure 13. For a broad range of thin joints, there was no effect of thickness, but very thick joints did display increased values of $\mathcal{G}_{ISCC}$. Even at these high values of $\mathcal{G}_{ISCC}$, fracturing continued to be IF.

CONCLUSIONS

1. Slow stable cracking of adhesive bonds under sustained loads requires both the presence of an aggressive environment and long time loading.

2. In short time loading, water increased the toughness of the bond whereas in long time loading the load carrying capacity of the bond is decreased by the presence of water.

3. Rapid cracking of adhesive bonds occurs cohesively, and, in bonds less than 25 mils thick, it occurs near the center of bond (CoB). It is only for such cohesive fracturing that water increases toughness.

4. In the presence of water, the long term application of loads less than the critical load corresponding to $\mathcal{G}_{IC}$ is likely to cause adhesive fracturing at the interface for the adhesive systems and adherend preparations studied. For such stress corrosion cracking there is a threshold value of $\mathcal{G}_{i}$, i.e., $\mathcal{G}_{ISCC}$, below which cracking will not occur.

5. The value of $\mathcal{G}_{ISCC}$ for a particular adhesive system is a function of relative humidity. As the humidity increases, $\mathcal{G}_{ISCC}$ decreases approaching as its lower limit the value of $\mathcal{G}_{ISCC}$ in liquid water containing a wetting agent.

6. If the adhesive bond can be kept dry (less than one percent R.H.), its load carrying capability for sustained loads is not reduced below its value of $\mathcal{G}_{IC}$.

7. The anhydride cured adhesive is more sensitive to SCC than the amine hardened one. Whereas the ratio of $\mathcal{G}_{ISCC}$ to $\mathcal{G}_{IC}$ for amine hardened joints was of the order of 1/2 to 1/4, this ratio for the anhydride system could be less than 1/10.

8. The value of $\mathcal{G}_{ISC}$ is independent of joint thickness up to 25 mils for the TEPA system and up to 100 mils for the HHPA system. For thicker joints $\mathcal{G}_{ISCC}$ increases.

9. The use of the TDCB specimen and the concepts of fracture mechanics provide a potential test procedure for evaluating the performance of adhesive bonds both for short time tests and under sustained loads in aggressive environments.

Acknowledgements

This program was carried out under a series of contracts with the Naval Air Systems Command. The authors gratefully acknowledge their permission to publish this work. The many helpful suggestions of G. R. Irwin, Lehigh University, H. T. Corten, University of Illinois, and R. L. Patrick, Alpha R & D, are also gratefully acknowledged.

References

1. S. Mostovoy, P. C. Crosley, and E. J. Ripling, *Journal of Materials*, **2**, 661 (1967).
2. S. Mostovoy and E. J. Ripling, *J. Appl. Poly. Sci.* **10**, 1351 (1966).
3. S. Mostovoy and E. J. Ripling, *J. Appl. Poly. Sci.* **13**, 1083 (1969).
4. E. J. Ripling, S. Mostovoy and H. T. Corten, this issue.
5. S. Mostovoy, C. Bersch and E. J. Ripling, this issue.
6. S. Mostovoy and E. J. Ripling, "Effect of Joint Geometry on the Toughness of Epoxy Adhesives", Section II, Final Report, Contract No. 00019-69-C-0231.
7. S. Mostovoy and E. J. Ripling, "Fracture Toughness and Stress Corrosion Cracking Characteristics of an Anhydride Hardened Epoxy Adhesive", Section I, Final Report, Contract No. 00019-69-C-0231.